Journal of Integrative Agriculture 2026, 25(8): 3218–3227

Available online at ScienceDirect

Journal of Integrative Agriculture

RESEARCH ARTICLE

Differential effects of daytime and nighttime high temperatures at the grain formation stage on starch structure and properties in waxy maize

Jing Li[1*], Xiaotian Gu[2*], Lingling Qu[1], Guanghao Li[1], Jian Guo[1], Dalei Lu[1, 3#]

[1] *Jiangsu Key Laboratory of Crop Genetics and Physiology/Jiangsu Co-Innovation Center for Modern Production Technology of Grain Crops/Agricultural College, Yangzhou University, Yangzhou 225009, China*

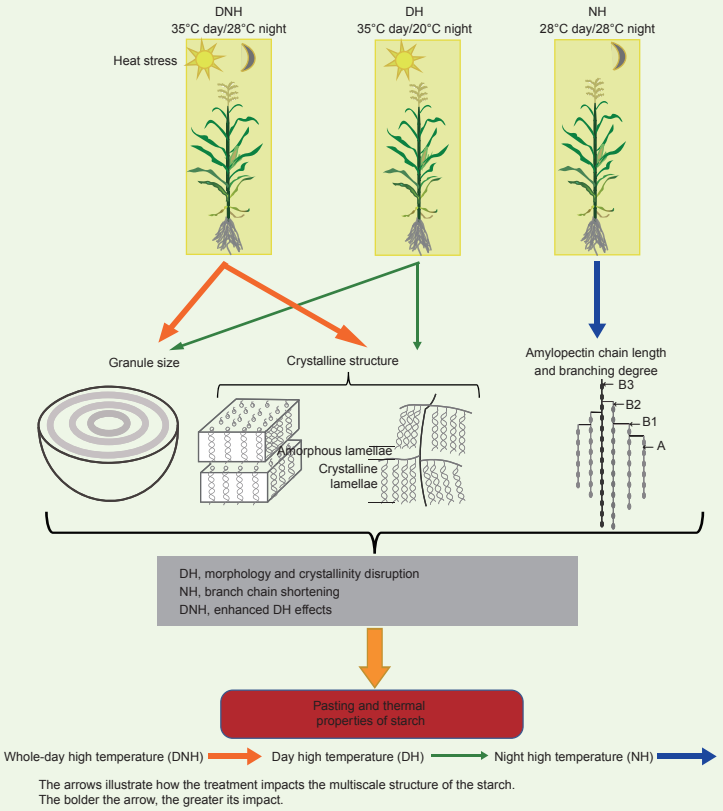
[2] *Yancheng Institute of Technology, Yancheng 224000, China*

[3] *Joint International Research Laboratory of Agriculture and Agri-Product Safety, Ministry of Education, Yangzhou 225009, China*

Highlights

- Day and night high temperature (DH and NH) stresses severely damage starch structure and quality, with DH having a greater impact.
- DH primarily affects starch granule size, relative crystallinity, and starch branching degree; NH primarily shortens amylopectin chains and retains more branching.
- Whole-day high temperature exerts a cumulative effect, causing more severe damage to starch than DH or NH.

Graphical abstract



Received 10 October 2024; Received in revised form 21 January 2025; Accepted 13 February 2025; Available online 20 March 2025
[#]Correspondence Dalei Lu, E-mail: dllu@yzu.edu.cn
[*] These authors contributed equally to this study.

© 2026 CAAS. Publishing services by Elsevier B.V. on behalf of KeAi Communications Co. Ltd. This is an open access article under the CC BY-NC-ND license (http://creativecommons.org/licenses/by-nc-nd/4.0/). Peer review under responsibility of Editorial Board of *Journal of Integrative Agriculture*.
doi: 10.1016/j.jia.2025.03.008

Abstract

High temperature (HT) is a critical abiotic stress factor that negatively impacts yield and quality of maize worldwide. Although the effects of HT during key growth stages are extensively documented, the distinct influences of daytime versus nighttime HT on the physicochemical properties of waxy maize starch remain largely unexplored. This study investigated the effects of daytime and nighttime HT on the on the starch physicochemical properties in two waxy maize hybirds. Temperature treatments included ambient temperature (NN), daytime HT (DH), nighttime HT (NH), and whole-day HT (DNH), which were applied from 1 to 15 days after pollination. The three HT stresses significantly inhibited starch synthesis and accumulation, increased the number of pores on the starch granule surface, enlarged starch granule size, enhanced relative crystallinity, and shortened the chain length and reduced the branching degree of amylopectin. The most severe effects were observed under DNH, followed by DH. DH and DNH reduced starch pasting viscosity and gelatinization enthalpy while increasing starch retrogradation through mechanisms involving enlargement of granule size, increased relative crystallinity, and reduced branching and chain length of amylopectin. NH increased gelatinization enthalpy and retrogradation and decreased starch pasting viscosity primarily by shortening the chain length of amylopectin. By elucidating the mechanisms through which daytime and nighttime HT affect starch physicochemical properties, this study provides valuable insights into optimizing waxy maize production in response to climate change challenges.

Keywords: waxy maize, high temperature, starch granule size, amylopectin chain length, pasting property, gelatinization property

1. Introduction

Starch is a primary carbohydrate source in human diets, providing essential energy for daily activities (Liu *et al.* 2021b). The biosynthesis of natural starch is a complex enzymatic process that critically determines its multiscale structure and physicochemical properties (Wang J *et al.* 2017). Research indicates that the pasting and thermal properties of starch are closely related to its multiscale structure, including granule morphology, crystalline form, and branched-chain structure (González *et al.* 2018; Liu *et al.* 2021a). Maize starch is the largest plant-based starch by proportion of global total starch production (Yu and Moon 2022). Among maize starches, normal maize starch comprises 23–28% amylose and 72–77% amylopectin, which imparts a low pasting viscosity and a high propensity for retrogradation, thereby limiting its application value (Waterschoot *et al.* 2014). Waxy maize (*Zea mays* L. var. *ceratina* Kulesh) is a distinctive maize type, as its starch is composed almost entirely of amylopectin. This composition confers high viscosity, minimal retrogradation, and excellent stability, making it ideal for use as a thickener, emulsifier, and binder in food, pharmaceutical, and industrial applications (Lu and Lu 2012; Ketthaisong *et al*. 2014; Klaochanpong *et al.* 2015; Sun *et al.* 2021).

Global temperatures have risen by approximately 1.1°C since the mid-19th century, with projections indicating an additional increase of 1.0 to 5.7°C by 2100 (Lynas *et al.* 2021; Gao and Cui 2023). This rise has led to more frequent extreme heat events, significantly threatening agricultural productivity and food quality, thereby posing substantial risks to global food security (Heino *et al.* 2023). In Southern China, high summer temperatures often coincide with critical stages of maize yield and quality development (Cao *et al.* 2024). Maize thrives at optimal temperatures, typically with daytime temperatures of 25–30°C and nighttime temperatures of 15–20°C (Yang *et al.* 2023). Favorable temperatures facilitate optimal photosynthetic activity, nutrient assimilation, and overall plant growth, ensuring high yield and good quality. Temperatures exceeding the optimal range, especially during critical growth stages like grain filling, severely impair development and productivity (Yang *et al.* 2023). During the grain-filling stages, high temperature (HT) suppresses the activities of key starch-synthesizing enzymes and enhances the activities of starch debranching and hydrolyzing enzymes, altering starch structural parameters, which impacts its function (Yang *et al.* 2018; Chi *et al.* 2021; Gu *et al.* 2022). Additionally, HT damages starch granules, disrupts crystalline structures, and breaks starch chains, leading to reduced viscosity and lower gelatinization temperatures (Gu *et al.* 2022; Wang *et al.* 2022; Lin *et al.* 2023). In our previous studies, we found that HT during 1–15 d after pollination (DAP) significantly affected grain development and yield in waxy maize, causing irreversible damage to starch synthesis (Lu *et al.* 2016; Gu *et al.* 2022).

Since the latter half of the 20th century, global minimum temperatures have increased more than twice as fast as maximum temperatures, revealing a significant day–night warming asymmetry across various regions (Wang K *et al.* 2017). Consequently, crop growth processes may be differentially affected by elevated daytime or nighttime temperatures. Carbohydrate accumulation in plants follows circadian rhythms, with sucrose and starch synthesized during the day and starch degraded at night (Kim *et al.* 2017). Previous studies on the effects of daytime or nighttime HT on crop growth have primarily focused on leaf photosynthesis, respiration, and overall yield (Kettler *et al.* 2022). However, knowledge of the different influences of daytime *vs*. nighttime HT on the starch quality of waxy maize grains remains limited. This study aims to elucidate the effects of daytime and/or nighttime HT on the quality of waxy maize starch from a multiscale structural perspective. We hypothesize that HT at different times of day alters starch structure at multiple scales, thereby differently affecting its physicochemical properties. The hybrids Suyunuo 5 (SYN5, heat-sensitive) and Yunuo 7 (YN7, heat-tolerant) were exposed to HT

conditions at the day (DH), night (NH), and whole-day (DNH) during 1–15 DAP. We assessed the multiscale structure and physicochemical properties of starch, as well as the activities of key enzymes involved in starch metabolism, to clarify the relationship between starch structure and its physicochemical properties. Our findings confirm the hypothesis and provide insights into optimizing waxy maize production in response to climate warming.

2. Materials and methods

2.1. Experiment design

In the spring of 2021, an experiment was conducted at the Yangzhou University Experimental Farm using two maize hybrids, SYN5 and YN7. Each pot, measuring 38 cm in height and 43 cm in diameter and containing 30 kg of sieved sandy loam soil, served as an experimental unit. Seedlings were initially germinated and nurtured in seeding trays in a greenhouse and transplanted into the pots upon the emergence of the first leaf. Three seedlings were initially placed in each pot, with only one retained at the jointing stage to ensure uniform growth. At the time of transplantation, each pot was fertilized with 10 g of compound fertilizer (N-P_2O_5-K_2O=15%–15%–15%). An additional 6.6 g of urea (46% N) was applied at the jointing stage. The plants were grown in a field setting until the silking stage, at which point manual pollination was conducted to ensure controlled fertilization. The following day, the pots were moved to a controlled-environment greenhouse for a 15-d temperature treatment period. The greenhouse (dimensions, 4 m×3 m; cooling/heating capacity, 115 kW; rated power input, 29 kW; supplied by Shanghai Yileng-Carrier Air Conditioning Equipment Co., Ltd., China) was set to the following temperature regimes: ambient temperature (NN, 28°C day/20°C night), daytime HT (DH, 35°C day/20°C night), nighttime HT (NH, 28°C day/28°C night), and whole-day HT (DNH, 35°C day/28°C night). After the 15-d temperature treatment, the greenhouse conditions were restored to ambient temperature settings until crop maturity, approximately 45 d after pollination. Uniform management practices, including watering and pest control, were maintained for all treated pots to ensure consistency across treatments. Each treatment group comprised 45 pots, allowing for robust statistical analysis of the effects of the different temperature regimes on maize growth and starch properties.

2.2. Starch content

At 5, 10, 15, 20, 25, 30, and 40 DAP, the kernels were removed from the ears and dried until a constant weight was achieved. The starch content at those stages was determined using the anthrone-sulfuric acid method after grinding the oven-dried kernels (Lu *et al.* 2014). Each treatment was conducted in triplicate.

2.3. Starch extraction

At maturity, three ears were harvested from each treatment of waxy maize plants. Grains from the central section of each ear were collected and homogenized. Approximately 100 g of homogenized grains were immersed in 0.5 L of 1 g L^{-1} $NaHSO_3$ solution at room temperature for 48 h. Starch extraction was performed following the method outlined by Lu *et al.* (2014). The isolated starch exhibited protein, lipid, and ash contents below 4, 2, and 2 mg g^{-1}, respectively, complying with the Chinese National Standard for edible maize starch (GB/T 8885–2017 2017). The starch was oven-dried at 45°C, sieved through a 100-mesh screen, and subsequently analyzed for its multiscale structure and physicochemical properties.

2.4. Starch granule morphology

The dried starch samples were observed using a scanning electron microscope (SEM). Starch granules were affixed to circular aluminum stubs using double-sided tape and sputtered with gold. The starch morphology was examined by SEM (GEMINI SEM 300, Carl Zeiss, Oberkochen, Germany) at an accelerating potential of 5 kV, and photographed at magnifications of 1,000× and 5,000×.

2.5. Granule size distribution

Starch granule size was measured using a laser diffraction particle size analyzer (Mastersizer 2000, Malvern, Worcestershire, England) (Lu *et al.* 2014). The instrument operates on the principle of laser diffraction, determining starch granule size by measuring the angle of scattered light. It can measure sizes ranging from 0.1 to 2,000 μm. Anhydrous alcohol was used as the dispersing medium, with the particle refractive index, particle absorption coefficient, and anhydrous alcohol refractive index set to 1.52, 0.10, and 1.32, respectively. Starch granule size data were collected and analyzed using Mastersizer 2000 v.5.20 software. The cumulative volumes of particles approaching 10, 50, and 90% were recorded as $d_{(v,\ 0.1)}$, $d_{(v,0.5)}$, and $d_{(v,0.9)}$, respectively. The size dispersion index (Span) was calculated using eq. (1):

$$Span=[d_{(v,0.9)}-d_{(v,0.1)}]/d_{(v,0.5)} \quad (1)$$

2.6. Molecular weight and amylopectin chain-length distributions

Starch samples were debranched using isoamylase dissolved in 50 mmol L^{-1} of NaAc. The molecular weight distribution was analyzed using a PL-GPC 220 high-temperature chromatograph (Agilent Technologies UK) equipped with three columns (PL110-6100, PL110-6300, and PL110-6525) and a differential refractive index detector (Cai *et al.* 2014).

The eluent system consisted of dimethyl sulfoxide containing 0.5 mmol L^{-1} of $NaNO_3$ at a flow rate of 0.8 mL min^{-1}. The column oven temperature was maintained at 80°C. Standard dextrans with known molecular weights (2,800, 18,500, 111,900, 410,000, 1,050,000, 2,900,000, and 6,300,000) were used for column calibration. Amylopectin chain-length distributions were analyzed *via* high-performance anion-exchange chromatography with pulsed amperometry detection (Liu *et al.* 2007). Technical support for molecular weight and amylopectin chain-length distributions was provided by Sanshu Biotech. Co., Ltd. (Shanghai, China). All experiments were performed in triplicate.

2.7. X-ray diffraction pattern

X-ray diffraction (XRD) patterns of the starch samples were

obtained using an X-ray diffractometer (D8 Advance, Bruker-AXS, Karlsruhe, Germany) (Yang *et al*. 2021). Relative crystallinity (RC, %) was calculated as the ratio of the total crystalline peak areas to the entire diffractogram (including both crystalline and amorphous peak areas) using MDI Jade 6 software. All experiments were conducted in triplicate.

2.8. Pasting property

The pasting properties were evaluated using a Rapid Viscosity Analyzer (RVA, Model 3D, Newport Scientific, Warriewood NSW, Australia). A total of 1.96 g of dried starch was weighed into an aluminum container, and 26.04 mL of distilled water was added, thoroughly mixing to form a 7% starch paste. The starch paste was heated to 95°C at a rate of 12°C min^{-1}, held at 95°C for 2.5 min, cooled to 50°C at the rate of 12°C min^{-1}, and maintained at 50°C for 1 min. The experiments were repeated three times.

2.9. Thermal property

Thermal characteristics of starch were analyzed using differential scanning calorimetry (DSC) (Model 200 *F3* Maia, NETZSCH, Bavaria, Germany). A total of 5 mg starch was placed into an aluminum crucible (25–40 μL, 5 mm in diameter). A total of 10 μL of distilled water was added and mixed evenly to form a 66.7% starch paste. The aluminum crucible was sealed and stored at 4°C for 24 h. The sample crucible was then heated from 20 to 100°C at a rate of 10°C min^{-1}, with an empty crucible serving as a reference. Thermal transitions of starch were characterized by onset temperature (T_o), peak gelatinization temperature (T_p), conclusion temperature (T_c), and gelatinization enthalpy (ΔH_{gel}). After thermal analysis, samples were stored at 4°C for 7 days to investigate retrogradation. Retrogradation enthalpy (ΔH_{ret}) was calculated automatically, and the retrogradation percentage (%R) was determined using the formula $\%R=(\Delta H_{ret}/\Delta H_{gel})\times100$. The experiments were repeated three times.

2.10. Activity of starch-metabolizing enzyme

The kernels from the middle of the ear were collected at 5, 10, 15, 20, 25, and 30 DAP and stored at –80°C. The activities of soluble starch synthase (SSS), sucrose synthase (SS), starch branching enzyme (SBE), starch debranching enzyme (SDBE), *α*-starch hydrolytic enzyme (*α*-SH), and *β*-starch hydrolytic enzyme (*β*-SH) were measured using enzyme-linked immunoassay reagent kits ml10983, ml10561, ml076664, ml10726, ml406923, and ml406961, respectively, from Shanghai Enzyme-linked Biotechnology Co., Ltd. (Shanghai, China). The experiments were repeated three times.

2.11. Statistical analysis and plotting

Experimental data were statistically analyzed using ANOVA in SPSS v. 26.0 (IBM, Armonk, NY, USA). Significant differences between treatments were identified at $P<0.05$. The figures were generated using SigmaPlot 14.0. Correlation coefficients were calculated using Pearson's method, and heatmaps were created using Origin 2021 (OriginLab, Massachusetts, USA).

3. Result

3.1. Starch accumulation in waxy maize grain

High temperature (HT) stress led to weakened activities of SSS, SS, SBE, and SDBE, and to enhanced activities of *α*-SH and *β*-SH in waxy maize grains (average from data at 5–30 DAP) (Fig. 1-A–F). The effects of different types of HT on enzyme activity followed the order DNH>DH>NH. Changes in enzyme activities related to starch synthesis under the HT treatment led to a decrease in starch content at 20–25 DAP (Fig. 1-G). At maturity, DH, NH, and DNH reduced starch content in SYN5 and YN7 grains, with reductions of 17.8, 10.1, and 15.9% in SYN5 and 15.5, 8.1, and 14.7% in YN7, respectively, compared to NN (Fig. 1-G).

3.2. Starch morphology and granules size

In comparison to NN, starch granules were enlarged and exhibited irregular shapes under DH, NH, and DNH treatments (Fig. 2-A–H). The HT treatment increased the number and diameter of pores on the granule surfaces. The effect was most pronounced under DNH, followed by DH (Fig. 2-A–H). Furthermore, the starch granules of SYN5 were more severely damaged than those of YN7. The granule size distribution of waxy maize starch displayed a bimodal pattern, ranging from 0.5 to 50 μm (Fig. 3). HT significantly affected the volume equivalent mean diameter ($D_{[4,3]}$) (Fig. 3) and the size dispersion index (Span) of starch granules in SYN5 and YN7 (Appendix A). Specifically, DH and DNH significantly increased $D_{[4,3]}$ in both hybrids ($P<0.05$) (Fig. 3), whereas NH had minimal impact. In YN7, the span significantly increased under HT, following the order DNH>NH>DH>NN. Similarly, DH significantly increased the span in SYN5 (Appendix A).

3.3. Starch multiscale structure

Crystalline structure of starch The X-ray diffraction (XRD) spectrum of waxy maize starch showed peaks at 15°, 17°, 18°, and 23° (Fig. 4). Except for SYN5 under NH, HT significantly increased the relative crystallinity (RC) of both hybrids, with RC increasing in the order DNH>DH>NH (Fig. 4).

Fine structure of starch Different HT stress types significantly affected the degree of polymerization (DP) of starch branches in waxy maize. Generally, HT stress led to a shortening of starch branches, with the order of reduction NH>DH>DNH, except for SYN5 under DNH (Fig. 5-A; Appendix B). Amylopectin chains are classified based on their DP into A chains (DP 6–12), B_1 chains (DP 13–24), B_2 chains (DP 25–36), and B_3 chains (DP≥37). HT treatments significantly altered the proportions of these different chains of starch branches. Specifically, the proportion of A chains followed the order NH>DH>NN>DNH; for B_1 chains, NH>DH=DNH>NN; for B_2 chains, NN>DH=DNH>NH; and for B_3 chains, NN>DH>DNH>NH (Fig. 5-B).

The molecular weight distribution of starch branches in SYN5 and YN7 was analyzed using gel permeation chromatography (GPC) after debranching with isoamylase. F1 represents the short branch chains (A and B1 chains), while F2 denotes long branch chains (B_2 and B_3 chains). The F1/F2 ratio serves as an indicator of the branching

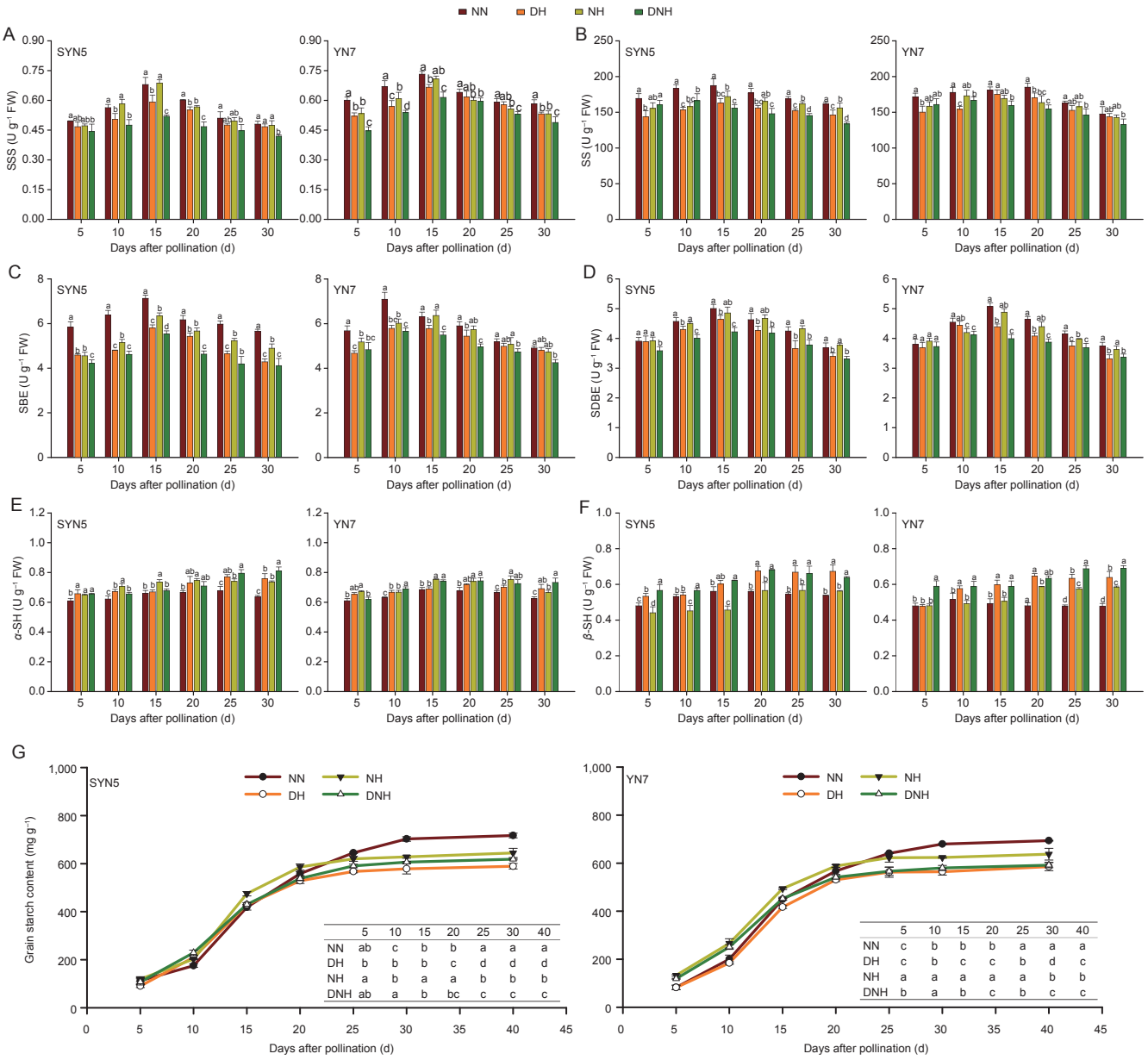


Fig. 1 Starch synthesis and accumulation of waxy maize under high daytime and/or nighttime temperatures at the grain formation stage. A, soluble starch synthase (SSS). B, sucrose synthase (SS). C, starch branching enzyme (SBE). D, starch debranching enzyme (SDBE). E, *α*-starch hydrolytic enzyme (*α*-SH). F, *β*-starch hydrolytic enzyme (*β*-SH). SYN5, Suyunuo 5; YN7, Yunuo 7. G, grain starch content at different growth stages of SYN5 and YN7. NN, ambient temperature; DH, day high temperature; NH, night high temperature; DNH, whole-day high temperature. Error bars represent the SD (*n*=3). Different letters among the four treatments at each stage indicate significant differences (P<0.05).

degree of amylopectin, where a lower ratio indicates fewer branch chains (Wu and Gilbert 2010). The results revealed that different HTs exerted distinct effects on the molecular weight of starch branches (Fig. 6-A). In SYN5, both DH and DNH significantly decreased the F1/F2 ratio, while NH had no effect. In YN7, all HTs reduced the F1/F2 ratio, with the degree of impact following the order NH<DH<DNH (Fig. 6-B).

3.4. Starch physicochemical properties

Starch pasting property HT significantly affected the pasting properties of waxy maize starch (Appendix C). The different HT stress types had varying impacts on the pasting characteristics of starch from the SYN5 and YN7. For SYN5, HT reduced the peak viscosity (PV), trough viscosity (TV), final viscosity (FV), breakdown viscosity (BD), and pasting temperature (P_{temp}), while setback viscosity (SB) significantly increased. The magnitude of these effects followed the order NH<DH<DNH (Table 1; Appendix C). Similarly, DH and DNH had comparable impacts on the pasting properties of YN7 starch, mirroring those observed in SYN5. In contrast, the NH did not cause significant changes in the pasting properties of YN7 starch.

Starch thermal property Changes in the multiscale structure of starch affected its thermal properties. Compared

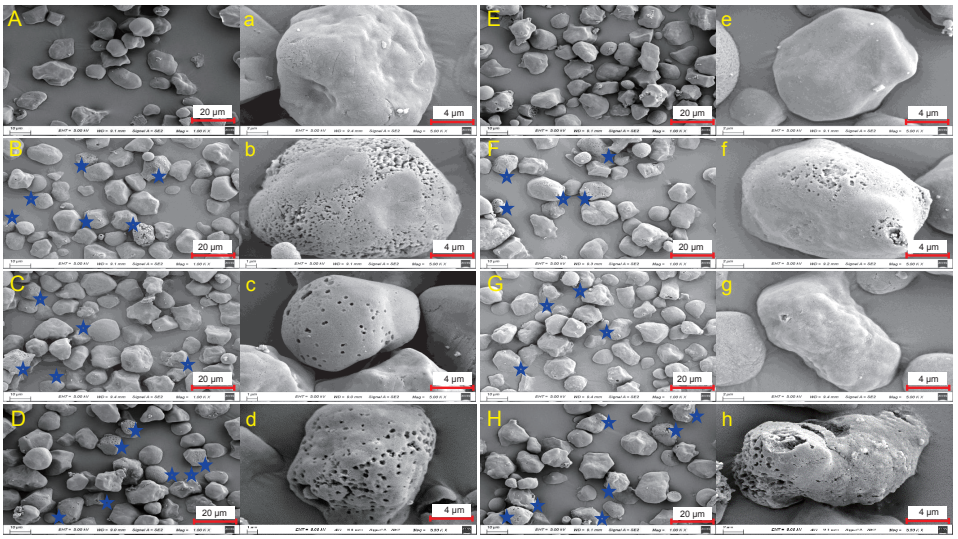


Fig. 2 Scanning electron micrographs of starch granules of waxy maize under high daytime and/or nighttime temperatures at the grain formation stage. A and a, Suyunuo 5 (SYN5) NN. B and b, SYN5 DH. C and c, SYN5 NH. D and d, SYN5 DNH. E and e, Yunuo 7 (YN7) NN. F and f, YN7 DH. G and g, YN7 NH. H and h, YN7 DNH. A–H, micrographs were taken at 1,000× magnification. a–h, micrographs were taken at 5,000× magnification. NN, ambient temperature; DH, day high temperature; NH, night high temperature; DNH, whole-day high temperature. Stars represent damaged starch granules.

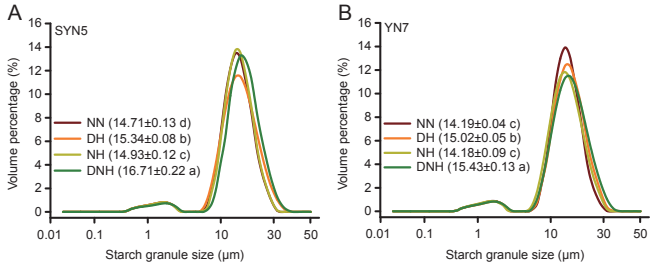


Fig. 3 Starch size and distribution under high daytime and/or nighttime temperatures at the grain formation stage. Data in brackets are the volume-equivalent mean diameter (μm), expressed by $D_{[4,3]}$. SYN5, Suyunuo 5; YN7, Yunuo 7. NN, ambient temperature; DH, day high temperature; NH, night high temperature; DNH, whole-day high temperature. Values are mean±SD (n=3). Different lowercase letters following the mean values for each hybrid indicate significant differences among four treatments (P<0.05).

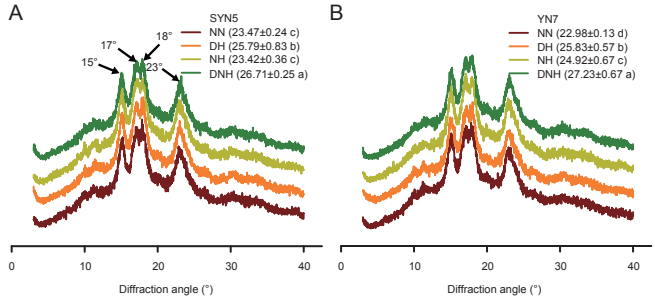


Fig. 4 X-ray diffraction profiles of starch under high daytime and/or nighttime temperatures at the grain formation stage. Data in brackets are relative crystallinity (RC, %). SYN5, Suyunuo 5; YN7, Yunuo 7. NN, ambient temperature; DH, day high temperature; NH, night high temperature; DNH, whole-day high temperature. Values are mean±SD (n=3). Different lowercase letters following the mean values for each hybrid indicate significant differences among four treatments (P<0.05).

to NN, DH and DNH resulted in a decrease in the ΔH_{gel} of starch. In contrast, NH led to an increase in ΔH_{gel}. All HT treatments (DH, NH, and DNH) caused an increase in both the ΔH_{ret} and the %R of starch, with the magnitude of the increase in %R following the order DH>NH>DNH (Table 2). Additionally, DH increased the gelatinization temperature of starch, whereas NH and DNH decreased it.

4. Discussion

4.1. Different HT stress types affect the morphology and size of waxy maize starch granules differentially

The period from 1 to 15 DAP in maize endosperm is characterized by cell differentiation, rapid cell division, and endoreduplication (Becraft and Gutierrez-Marcos 2012; Leroux *et al.* 2014; Li *et al.* 2023). After 15 DAP, cell proliferation ceases, and the endosperm transitions into a phase of rapid starch accumulation (Liu *et al.* 2022). The number and size of endosperm cells significantly influence starch accumulation and the morphology of granules, which in turn affect the multiscale structure and physicochemical properties of starch. During 1–15 DAP, HT stress limited kernel starch accumulation, resulting in an increased proportion of damaged starch granules and enlarged granule size ($D_{[4,3]}$) (Figs. 1 and 2). These changes affected the pasting and thermal properties of the starch (Lu *et al.* 2014; Gu *et al.* 2022) and made the starch granules more susceptible to mechanical damage from friction and impact, thereby reducing their functional value (Xu *et al.* 2020). In this study, different HT stress types had varying effects on the $D_{[4,3]}$, primarily due to differences in the distribution proportions of starch granules. Under DH and DNH stress, the $d_{(v,0.5)}$ and $d_{(v,0.9)}$ of starch granules in SYN5 and YN7

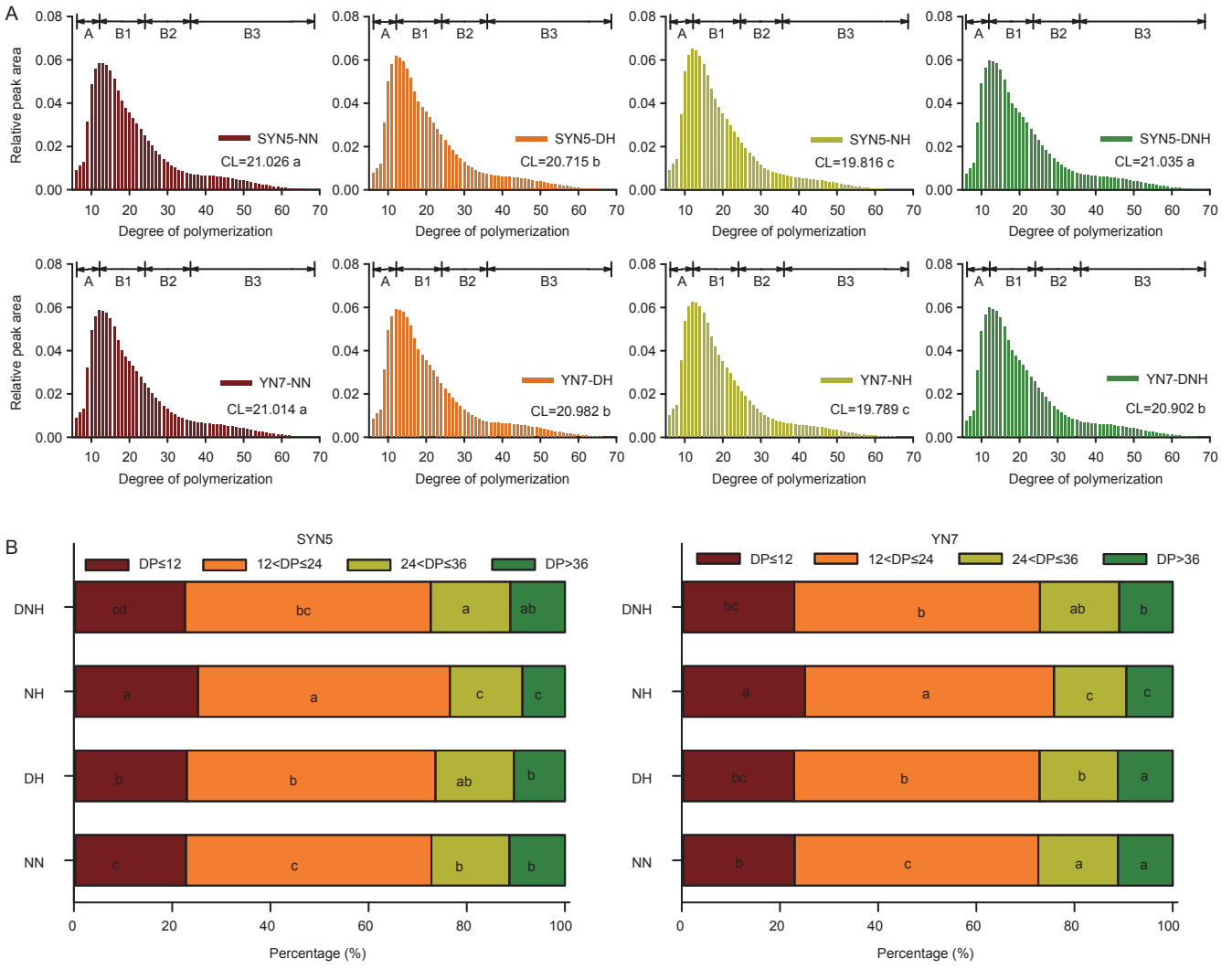


Fig. 5 Amylopectin chain-length distributions of starch under high daytime and/or nighttime temperatures at the grain formation stage. A, starch amylopectin chain-length distributions. CL, average chain length. B, percentages of chain lengths with degree of polymerization (DP)≤12, 13<DP≤24, 24<DP≤36, and DP>36. SYN5, Suyunuo 5; YN7, Yunuo 7. NN, ambient temperature; DH, day high temperature; NH, night high temperature; DNH, whole-day high temperature. Different lowercase letters indicate significant differences among four treatments (P<0.05).

increased, leading to an enlarged size. This was mainly attributed to HT affecting amyloplast development, reducing starch granule number and enlarging granule size (Lu *et al.* 2014). Additionally, HT stress caused insufficient assimilate supply during the later stages of kernel development (Hu *et al.* 2023), leading to an increased proportion of small-diameter starch granules. Conversely, NH stress primarily limited the supply of assimilates to kernels, affecting starch accumulation (Shi *et al.* 2017; Lal *et al.* 2022).

4.2. Different HT stress types affect the starch multiscale structure of waxy maize differentially

In starch, the branched chains (10<DP<25) intertwine into double-helical structures, which link end-to-end to create ring structures that are orderly arranged to establish the crystalline architecture (Zhu and Liu 2020). The free branched chains form the amorphous regions of the starch granules (Chi *et al.* 2021). After HT stress, no significant changes were observed in the XRD peaks at 15°, 17°, 18°, and 23°, but the RC significantly increased (Fig. 4). This indicated that HT stress did not alter the starch crystallization pattern (Pfister *et al.* 2020; Liu *et al.* 2021a), but affected the ratio of the crystalline and amorphous regions (Lin *et al.* 2020; Gu *et al.* 2022). The primary reason is that HT enhanced the activity of starch hydrolases (*α*-SH and *β*-SH) (Fig. 1), promoting the cleavage of side chains in the amorphous regions and thereby increasing the RC (Appendix D) (Chen *et al.* 2024). Among different types of HT treatments, NH had a minimal effect on RC, indicating that HT is more severe during the daytime than during the nighttime.

In this study, HT reduced the average chain length, which was primarily attributed to an increased proportion of A and B_1 chains and a concomitant decrease in B_2 and B_3 chains (Fig. 5). The formation and elongation of amylopectin branches in waxy maize starch are complex enzymatic processes, influenced by the activities of key

enzymes involved in starch biosynthesis and the content of disaccharides (Chi *et al.* 2021). HT stress decreased the carbon assimilate content in kernels (Impa *et al.* 2019) and reduced the activities of SS and SSS (Fig. 1), thereby limiting branch elongation and increasing the proportions of A and B_1 chains (Appendix D) (Chi *et al.* 2021). Notably, the activities of SBE and SDBE in the NH were higher than those in DH and DNH, resulting in a greater number of starch branches and a higher proportion of A and B_1 chains (Appendix D; Fig. 5-B). Additionally, HT stress elevated the activities of *α*-SH and *β*-SH, which promoted the hydrolysis of B_2 and B_3 chains into free maltose, maltotriose, and dextrin (Lin *et al.* 2023), resulting in shorter chain lengths (Figs. 1 and 5).

HT stress led to a reduction in the molecular weight and F1/F2 ratio of waxy maize starch branches, with the magnitude of decrease following the order NH<DH<DNH (Fig. 6). The decrease in branching can be attributed to reduced activities of SS, SSS, SBE, and SDBE under all HT stresses (Fig. 1), which limits the formation and extension of new branch chains and consequently reduces the number of branches (Lin *et al.* 2023). NH had the smallest impact on enzyme activity, resulting in the smallest decrease in starch branching degree (F1/F2) (Fig. 6-B). In addition, the decrease in the average chain length of starch also led to a reduction in molecular weight (Figs. 5 and 6-A).

4.3. Different HT stress types affect the physicochemical properties of waxy maize starch differentially

In the present study, HT stress resulted in decreased starch pasting viscosities (PV, TV, FV, and BD) and P_{temp} and increased SB. The starch pasting characteristics are closely linked to its multiscale structure. Despite the increase in RC observed under HT stress, molecular forces and branch chain lengths decreased. These structural modifications weakened water absorption and swelling capacities during the gelatinization process, leading to decreased pasting viscosities (Liu *et al.* 2021a; Wang *et al.* 2022). The SB of both hybrids significantly increased under HT stress, suggesting that HT reduced the stability of starch pasting, adversely affecting the starch functional properties in food utilization. YN7 exhibited a smaller decrease in starch pasting viscosities in NH than in NN. This may be attributed to its lesser impact on the RC and starch branching degree.

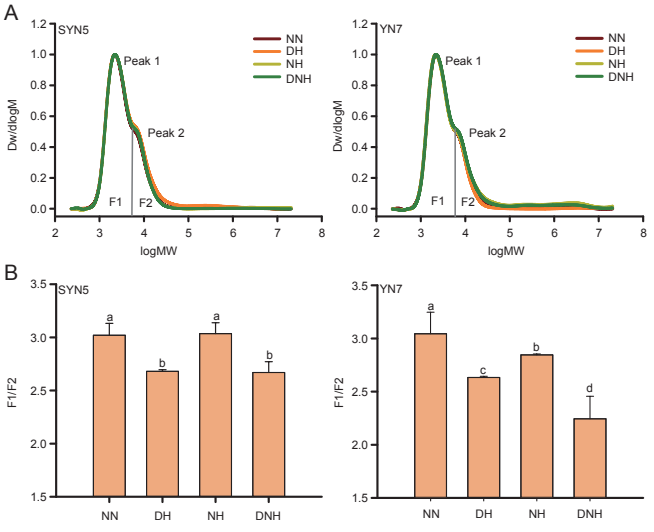


Fig. 6 Amylopectin molecular weight distribution of starch under high daytime and/or nighttime temperatures at the grain formation stage. A, gel permeation chromatography profiles of isoamylase debranched starch. B, F1/F2, the ratio of the F1 peak area to the F2 peak area, indicating the branching degree of amylopectin. SYN5, Suyunuo 5; YN7, Yunuo 7. NN, ambient temperature; DH, day high temperature; NH, night high temperature; DNH, whole-day high temperature. MW, molecular weight; Dw, differential weight. Different lowercase letters above the bars indicate significant differences among four treatments (P<0.05).

Changes in the starch multiscale structure affect its thermodynamic properties. In this study, DH and DNH led to decreases in the ΔH_{gel} of both SYN5 and YN7, while their RCs significantly increased. The result contrasts with previous conclusions that starch RC is positively correlated with ΔH_{gel}. This discrepancy may be attributed to DH and DNH, which cause starch granule enlargement and increase surface porosity, enhancing water molecule penetration and making the crystalline regions more susceptible to disruption, thereby reducing the energy required for gelatinization (Maldaner *et al.* 2021). This also explains the decreased gelatinization temperatures (T_o, T_p, and T_c) observed in DNH. NH increased the gelatinization enthalpy and temperatures in both hybrids. This can be primarily attributed to the minimal impact of NH stress on starch granule morphology, resulting in a more stable crystalline structure that requires more energy for gelatinization. Moreover, compared to NN, DH, NH, and DNH all led to significant increases in the ΔH_{ret} and %R of the starches. The shorter branch chains are more prone to rearrangement and formation of crystalline structures during the cooling process, leading to increased retrogradation (Fig. 5) (Lin *et al.* 2023). HT stress increases the retrogradation of waxy maize starch during food processing, thereby generating new utilizations.

4.4. Application of the HT stressed waxy maize starch

In the context of global climate change, the production and quality of waxy maize starch are severely affected (Yang *et al.* 2018; Chi *et al.* 2021; Gu *et al.* 2022; Heino *et al.* 2023). The findings of this study offer critical insights into how different types of HT stress influence the multiscale structure and physicochemical properties of waxy maize starch, which are crucial for its value in food and industrial sectors. A decrease in pasting viscosity of starch under HT conditions affects the quality and stability of waxy maize starch during food processing (Liu *et al.* 2021b). The reduction in molecular weight and degree of branching of starch under HT conditions potentially enhances its hydrolysis rate, thus improving starch conversion efficiency in industrial applications (Lin *et al.* 2024). However, these alterations diminish starch's applicability in the production of high-quality adhesives and biodegradable plastics (Zhang *et al.* 2015). Therefore, understanding the impact of various HT stresses on starch structure and properties is crucial for producing high-quality starch under future climate scenarios.

Table 1 Effect of high daytime and/or nighttime temperatures at the grain formation stage on pasting characteristics of waxy maize[1)]

Hybrids[2)]	Treatment[3)]	PV (cP)	TV (cP)	BD (cP)	FV (cP)	SB (cP)	P_{temp} (°C)
SYN5	NN	2,193±46 a	1,150±42 a	1,042±23 a	1,198±21 a	47.0±7.8 b	79.7±0.5 a
	DH	1,625±32 b	947±26 b	679±10 c	997±27 b	50.0±7.8 b	78.4±0.7 ab
	NH	1,632±20 b	953±24 b	678±17 c	1,011±28 b	57.0±10.4 b	78.4±0.9 ab
	DNH	1,525±17 c	845±27 c	712±76 b	935±65 c	89.3±15.5 a	77.3±1.0 b
YN7	NN	2,139±62 a	1,142±33 a	997±35 a	1,198±23 a	56.3±19.3 a	78.4±0.9 a
	DH	1,753±65 b	984±31 b	769±35 b	1,043±13 c	59.3±10.0 a	77.1±0.4 b
	NH	2,036±67 a	1,080±43 a	956±66 a	1,128±47 b	58.0±8.9 a	78.3±0.1 a
	DNH	1,349±49 c	647±27 c	702±24 c	709±18 d	61.7±9.3 a	77.9±1.3 b

[1)] PV, peak viscosity; TV, trough viscosity; BD, breakdown viscosity; FV, final viscosity; SB, setback viscosity; P_{temp}, pasting temperature.
[2)] SYN5, Suyunuo 5; YN7, Yunuo 7.
[3)] NN, ambient temperature; DH, daytime high temperature; NH, nighttime high temperature; DNH, whole-day high temperature.
Values are mean±SD (n=3). Mean value in the same column within each hybrid, followed by different letters, is significantly different (P<0.05).

Table 2 Effects of high daytime and/or nighttime temperatures at the grain formation stage on thermal characteristics of waxy maize starch[1)]

Hybrids[2)]	Treatment[3)]	ΔH_{gel} (J g^{-1})	T_o (°C)	T_p (°C)	T_c (°C)	ΔH_{ret} (J g^{-1})	%R
SYN5	NN	12.0±0.1 ab	69.3±0.1 c	74.3±0.0 b	82.7±0.3 bc	4.9±0.0 b	40.6±0.4 d
	DH	11.6±0.5 bc	73.3±0.1 a	77.1±0.2 a	84.5±0.3 a	6.2±0.2 a	54.0±0.35 a
	NH	12.5±0.3 a	69.9±0.2 b	73.8±0.1 c	83.4±0.5 b	6.5±0.5 a	51.6±1.9 b
	DNH	10.9±0.7 c	67.5±0.7 d	73.6±0.2 c	81.9±0.0 c	5.1±0.0 b	47.1±2.8 c
YN7	NN	11.2±0.0 b	67.9±0.3 b	73.7±0.1 c	80.7±0.0 b	4.7±0.0 d	41.6±0.2 c
	DH	10.8±0.8 c	69.7±0.3 a	74.5±0.6 b	84.0±0.9 ab	6.5±0.3 b	60.5±0.9 a
	NH	13.9±0.4 a	69.7±0.2 a	75.2±0.4 a	84.9±0.1 a	7.3±0.4 a	52.6±1.6 b
	DNH	10.9±0.4 c	69.4±0.1 a	73.8±0.1 c	80.2±0.3 b	5.6±0.1 c	51.5±0.8 b

[1)] ΔH_{gel}, gelatinization enthalpy; T_o, onset temperature; T_p, peak gelatinization temperature; T_c, conclusion temperature; ΔH_{ret}, retrogradation enthalpy; %R, retrogradation percentage.
[2)] SYN5, Suyunuo 5; YN7, Yunuo 7.
[3)] NN, ambient temperature; DH, daytime high temperature; NH, nighttime high temperature; DNH, whole-day high temperature.
Values are mean±SD (n=3). Mean value in the same column within each hybrid, followed by different letters, is significantly different (P<0.05).

5. Conclusion

High temperature stress alters the multiscale structure of waxy maize starch by directly affecting starch biosynthesis. DH primarily modifies starch granule morphology, enlarges granule size and increases RC, reduces the branching degree, and shortens the amylopectin chain length. These modifications result in decreased starch pasting viscosity and gelatinization enthalpy, but increased starch retrogradation. In contrast, NH mainly shortens the amylopectin chain length while maintaining a high branching degree. NH decreases the starch pasting viscosity but increases gelatinization enthalpy and retrogradation values. The impact on the starch physicochemical properties under NH was less than that under DH. The effects of DNH on starch structural and physicochemical properties are similar to those of DH but are more pronounced. The findings elucidate the differential impacts of daytime and/or nighttime HT on the structural and physicochemical properties of waxy maize starch, providing a solid theoretical basis for improving its application and quality under future climate variability.

Acknowledgements

This study was supported by the National Natural Science Foundation of China (32071958, 31771709, and 32372222), the Priority Academic Program Development of Jiangsu Higher Education Institutions, China.

Declaration of competing interest

The authors declare that they have no conflict of interest.

Declaration of generative AI and AI-assisted technologies in the writing process

The authors declare that they did not use AI in the preparation and writing of this manuscript.

Appendices associated with this paper are available at https://doi.org/10.1016/j.jia.2025.03.008

References

Becraft P W, Gutierrez-Marcos J. 2012. Endosperm development: Dynamic processes and cellular innovations underlying sibling altruism. *Wiley Interdisciplinary Reviews* (Developmental Biology), **1**, 579–593.

Cai J W, Cai C H, Man J M, Zhou W D, Wei C X. 2014. Structural and functional properties of C-type starches. *Carbohydrate Polymers*, **101**, 289–300.

Chen R, Zhao J J, Sui Z Q, Danino D, Corke H. 2024. Comparative analysis of granular starch hydrolysis and multi-structural changes by diverse α-amylases sources: Insights from waxy rice starch. *Food Chemistry*, **444**, 138622.

Chi C C, Li X X, Zhang Y P, Chen L, Li L, Miao S. 2021. Progress in tailoring starch intrinsic structures to improve its nutritional value. *Food Hydrocolloids*, **113**, 106447.

Cao C, Guan X, Li C, Gao Z, Gu T. 2024. Anthropogenic contribution to the unprecedented 2022 midsummer extreme high-temperature event in southern china. *Bulletin of the American Meteorological*

Society, **105**, 233–238.
Gao L, Cui X F. 2023. Climate change and food security: Plant science roles. *Molecular Plant*, **16**, 1481–1483.
GB/T 8885-2017. 2017. *Edible Corn Starch*. National Standard of the People's Republic of China. (in Chinese)
González L C, Loubes M A, Tolaba M P. 2018. Incidence of milling energy on dry-milling attributes of rice starch modified by planetary ball milling. *Food Hydrocolloids*, **82**, 155–163.
Gu X T, Zhang X Y, Lu W P, Lu D L. 2022. Starch structural and functional properties of waxy maize under different temperature regimes at grain formation stage. *Food Chemistry* (X), **16**, 100463.
Heino M, Kinnunen P, Anderson W, Ray D K, Puma M J, Varis O, Siebert S, Kummu M. 2023. Increased probability of hot and dry weather extremes during the growing season threatens global crop yields. *Scientific Reports*, **13**, 3583.
Hu J, Zhao X Y, Gu L M, Liu P, Zhao B, Zhang J W, Ren B Z. 2023. The effects of high temperature, drought, and their combined stresses on the photosynthesis and senescence of summer maize. *Agricultural Water Management*, **289**, 108525.
Impa S M, Vennapusa A R, Bheemanahalli R, Sabela D, Boyle D, Walia H, Jagadish S V K. 2019. High night temperature induced changes in grain starch metabolism alters starch, protein, and lipid accumulation in winter wheat. *Plant, Cell & Environment*, **43**, 431–447.
Ketthaisong D, Suriharn B, Tangwongchai R, Lertrat K. 2014. Changes in physicochemical properties of waxy corn starches after harvest, and in mechanical properties of fresh cooked kernels during storage. *Food Chemistry*, **151**, 561–567.
Kettler B A, Carrera C S, Nalli Sonzogni F D, Trachsel S, Andrade F H, Neiff N. 2022. High night temperature during maize post-flowering increases night respiration and reduces photosynthesis, growth and kernel number. *Journal of Agronomy and Crop Science*, **208**, 335–347.
Kim J, Kim H S, Choi S H, Jang J Y, Jeong M J, Lee S. 2017. The importance of the circadian clock in regulating plant metabolism. *International Journal of Molecular Sciences*, **18**, 2680.
Klaochanpong N, Puttanlek C, Rungsardthong V, Puncha-arnon S, Uttapap D. 2015. Physicochemical and structural properties of debranched waxy rice, waxy corn and waxy potato starches. *Food Hydrocolloids*, **45**, 218–226.
Lal M K, Sharma N, Adavi S B, Sharma E, Altaf M A, Tiwari R K, Kumar R, Kumar A, Dey A, Paul V, Singh B, Singh M P. 2022. From source to sink: Mechanistic insight of photoassimilates synthesis and partitioning under high temperature and elevated [CO_2]. *Plant Molecular Biology*, **110**, 305–324.
Leroux B M, Googyke A J, Schumacher K I, Abbott C P, Clore A M, Yagegari R, Larkins B A, Dannrnhoffer J M. 2014. Maize early endosperm growth and development: From fertilization through cell type differentiation. *American Journal of Botany*, **101**, 1259–1274.
Li X C, Wu J, Yi F, Lai J S, Chen J. 2023. High temporal-resolution transcriptome landscapes of maize embryosac and ovule during early seed development. *Plant Molecular Biology*, **111**, 233–248.
Lin C L, Lin J H, Pan C L, Chang Y H. 2024. Weakening the integrity of waxy starch granules by selective degradation of amorphous matrices using gaseous hydrogen chloride. *Carbohydrate Polymers*, **329**, 121793.
Lin G, Yang Y, Chen X Y, Yu X R, Wu Y F, Xiong F. 2020. Effects of high temperature during two growth stages on caryopsis development and physicochemical properties of starch in rice. *International Journal of Biological Macromolecules*, **145**, 301–310.
Lin H T, Yeh A I, Ho T H D, Pan M H, Chen S H. 2023. Molecular weight, chain length distribution and long-term retrogradation of cassava starch modified by amylomaltase. *Food Hydrocolloids*, **134**, 108027.
Liu C C, Jiang Y, Liu J D, Li K, Li J B. 2021a. Insights into the multiscale structure and pasting properties of ball-milled waxy maize and waxy rice starches. *International Journal of Biological Macromolecules*, **168**, 205–214.
Liu C C, Li K, Li X X, Zhang M J, Li J B. 2021b. Formation and structural evolution of starch nanocrystals from waxy maize starch and waxy potato starch. *International Journal of Biological Macromolecules*, **180**, 625–632.
Liu J X, Wu M W, Liu C M. 2022. Cereal endosperms: Development and storage product accumulation. *Annual Review of Plant Biology*, **73**, 255–291.
Liu Q, Gu Z, Donner E, Tetlow I, Emes M. 2007. Investigation of digestibility in vitro and physicochemical properties of A- and B-type starch from soft and hard wheat flour. *Cereal Chemistry*, **84**, 15–21.
Lu D L, Lu W P. 2012. Effects of protein removal on the physicochemical properties of waxy maize flours. *Starch-Stärke*, **64**, 874–881.
Lu D L, Shen X, Cai X M, Yan F B, Lu W P, Shi Y C. 2014. Effects of heat stress during grain filling on the structure and thermal properties of waxy maize starch. *Food Chemistry*, **143**, 313–318.
Lu D L, Yang H, Shen X, Lu W P. 2016. Effects of high temperature during grain filling on physicochemical properties of waxy maize starch. *Journal of Integrative Agriculture*, **15**, 309–316.
Lynas M, Houlton B Z, Perry S. 2021. Greater than 99% consensus on human caused climate change in the peer-reviewed scientific literature. *Environmental Research Letters*, **16**, 114005.
Maldaner V, Coradi P C, Nunes M T, Müller A, Carneiro L O, Teodoro P E, Ribeiro T, Bressiani J, Anschau K F, Müller E I. 2021. Effects of intermittent drying on physicochemical and morphological quality of rice and endosperm of milled brown rice. *LWT-Food Science and Technology*, **152**, 112334.
Pfister B, Zeeman S C, Rugen M D, Field R A, Ebenhoh O, Raguin A. 2020. Theoretical and experimental approaches to understand the biosynthesis of starch granules in a physiological context. *Photosynthesis Research*, **145**, 55–70.
Shi W J, Xiao G, Struik P C, Jagadish K S V, Yin X Y. 2017. Quantifying source–sink relationships of rice under high night-time temperature combined with two nitrogen levels. *Field Crops Research*, **202**, 36–46.
Sun Z H, Kang J, Shi Y C. 2021. Changes in molecular size and shape of waxy maize starch during dextrinization. *Food Chemistry*, **348**, 128983.
Wang H W, Wang Y, Xu K, Zhang Y Y, Shi M M, Liu X L, Chi C C, Zhang H. 2022. Causal relations among starch hierarchical structure and physicochemical characteristics after repeated freezing-thawing. *Food Hydrocolloids*, **122**, 107121.
Wang J, Hu P, Chen Z C, Liu Q Q, Wei C X. 2017. Progress in high-amylose cereal crops through inactivation of starch branching enzymes. *Frontiers in Plant Science*, **8**, 469.
Wang K, Li Y G, Wang Y, Yang X Y. 2017. On the asymmetry of the urban daily air temperature cycle. *Journal of Geophysical Research-Atmospheres*, **122**, 5625–5635.
Waterschoot J, Gomand S V, Fierens E, Delcour J A. 2014. Production, structure, physicochemical and functional properties of maize, cassava, wheat, potato and rice starches. *Starch-Stärke*, **67**, 14–29.
Wu A C, Gilbert R G. 2010. Molecular weight distributions of starch branches reveal genetic constraints on biosynthesis. *Biomacromolecules*, **11**, 3539–3547.
Xu J C, Chen L, Guo X B, Liang Y, Xie F W. 2020. Understanding the multi-scale structure and digestibility of different waxy maize starches. *International Journal of Biological Macromolecules*, **144**, 252–258.
Yang H, Gu X T, Ding M Q, Lu W P, Lu D L. 2018. Heat stress during grain filling affects activities of enzymes involved in grain protein and starch synthesis in waxy maize. *Scientific Reports*, **8**, 15665.
Yang H, Wei Q, Lu W P, Lu D L. 2021. Effects of post-silking low temperature on the physicochemical properties of waxy maize starch. *International Journal of Biological Macromolecules*, **188**, 160–168.
Yang Z, Cao Y, Shi Y, Qin F, Jiang C, Yang S. 2023. Genetic and molecular exploration of maize environmental stress resilience: Toward sustainable agriculture. *Molecular Plant*, **16**, 1496–1517.
Yu J K, Moon Y S. 2022. Corn starch: Quality and quantity improvement for industrial uses. *Plants*, **11**, 92.
Zhang Y H, Ding L L, Gu J Y, Tan H Y, Zhu L B. 2015. Preparation and properties of a starch-based wood adhesive with high bonding strength and water resistance. *Carbohydrate Polymers*, **115**, 32–37.
Zhu F, Liu P Z. 2020. Starch gelatinization, retrogradation, and enzyme susceptibility of retrograded starch: Effect of amylopectin internal molecular structure. *Food Chemistry*, **316**, 126036.

Executive Editor-in-Chief Shaokun Li
Managing Editor Ning Wang